CHAPTER – 6

INVERSE HALL PETCH EFFECT IN NANOCRYSTALLINE Al_5Fe_2 INTERMETALLIC

Chapter – 6

INVERSE HALL PETCH EFFECT IN NANOCRYSTALLINE Al_5Fe_2 INTERMETALLIC

In case of Al-Fe system, no systematic study on intermetallic phases in view of mechanical behavior in particular hardness was done except for MA Al-20 at.%Fe alloy which indicated a decrease in Hall-Petch slope with milling time indicating transition from hardening to softening [Nayak *et al.* (2010)]. Hence an effort has been made to synthesize single equilibrium intermetallic orthorhombic Al_5Fe_2 phase from Al-30 at.% Fe alloy and subjecting them to mechanical milling to obtain a better understanding on the evolution of phases with milling time and the effect of these phases on the mechanical properties of the alloy.

6.1 Structural evolution during milling

The characteristic X-ray diffraction pattern of as-cast powders of Al-30 at.% Fe alloy is shown in Fig. 6.1. The most intense diffraction peak (2 2 1) and (3 1 1) at 2θ = 42.55 and 43.79, was found in the as-cast alloy. JCPDS data suggests that this compound is representative of single Al_5Fe_2 orthorhombic phase (JCPDS 00-047-1435) with lattice parameters of a = 0.7648 nm, b = 0.6413 nm and c = 0.4216 nm. Results of XRD patterns showing structural evolution of Al_5Fe_2 intermetallic subjected to MM for different ranges of milling time are shown in Fig. 6.2. It is apparent that milling up to 30 h disappearance of all peaks except for major peaks of (2 2 1) and (3 1 1) was observed. The broadening observed in the diffraction peak, can be attributed to the major peaks overlapping from the intermetallic phase. The results obtained are in

contrary to Al_5Fe_2 obtained by MA route [Mukhopadhyay *et al.* (1995)], where complete formation of intermetallic phase was achieved in Al-25%Fe after 30 h of MA and the formation of amorphous phase was seen after 50 h of MA. Further in a similar work, Hunag *et al.* (1997) observed the formation of the Al_5Fe_2 intermetallic in nominally Al-24.4%Fe powder heat treated at 500°C after MA for 180 h. It is interesting to note that the XRD peaks undergo broadening in the course of mechanical milling up to 50 h mainly due to cumulative effects of grain refinement and lattice strain. The crystallite size decreased to about 10 nm during varying stages of milling from 10 to 50 h where as strain induced varied from 0.52 % to 0.65 % for 10 to 50 h, as shown in Fig. 6.3.

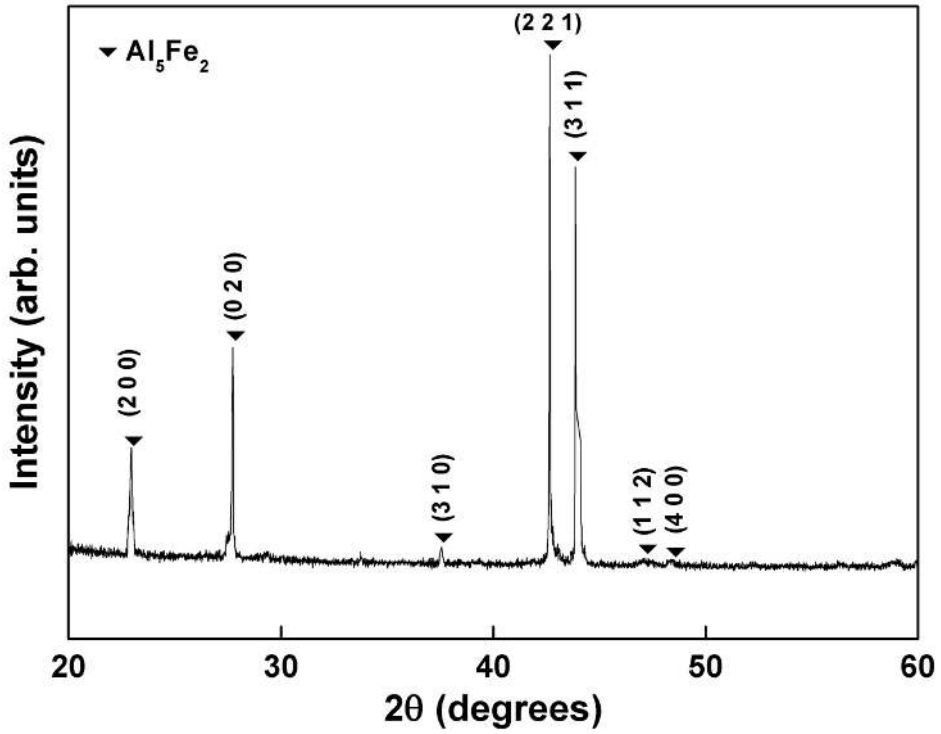

Figure 6.1: XRD pattern of as-cast of Al-30 at.% Fe alloy.

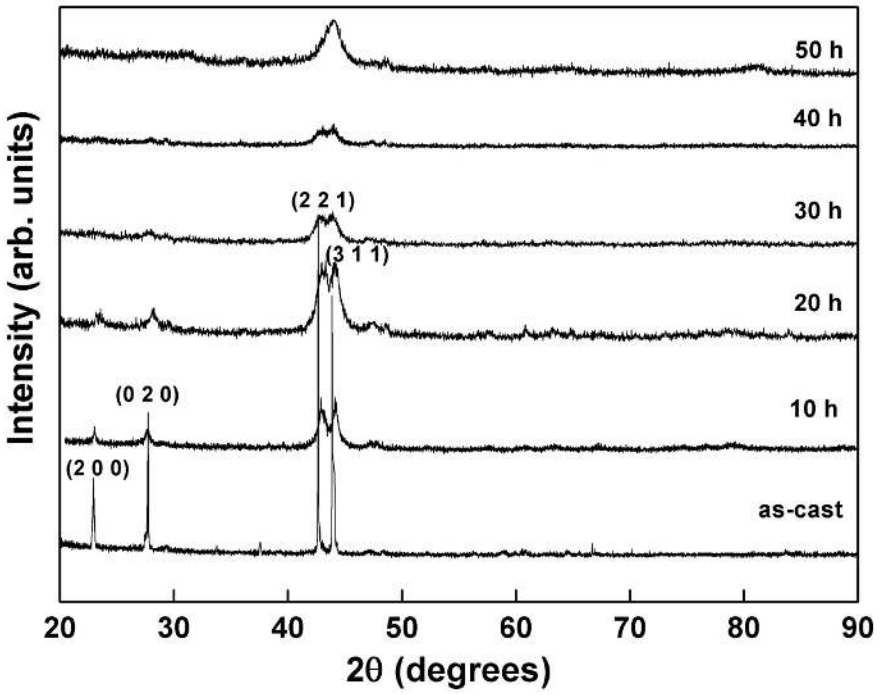

Figure 6.2: XRD patterns showing structural evolution of Al_5Fe_2 intermetallic during MM.

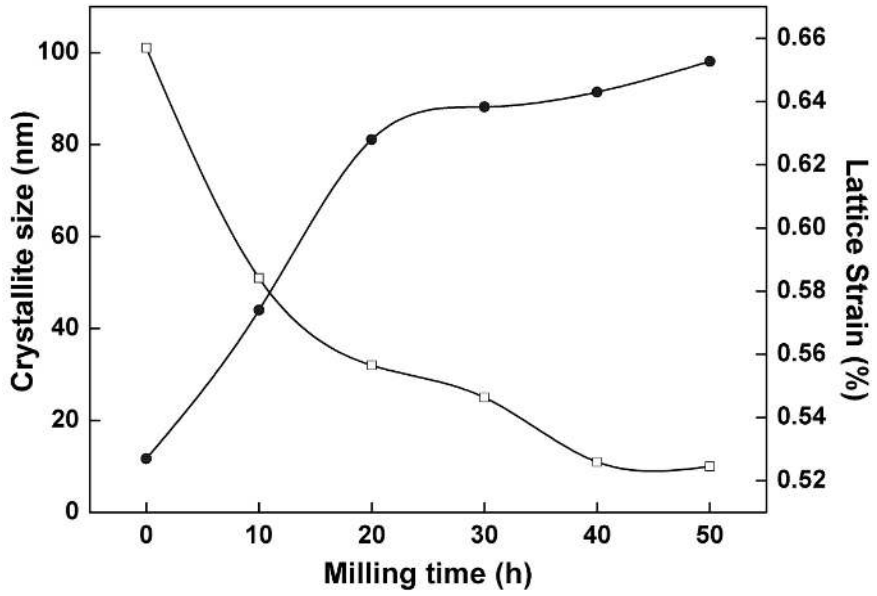

Figure 6.3: Variation of crystallite size and lattice strain for Al_5Fe_2 intermetallic as a function of milling time.

6.2 Morphological characteristics

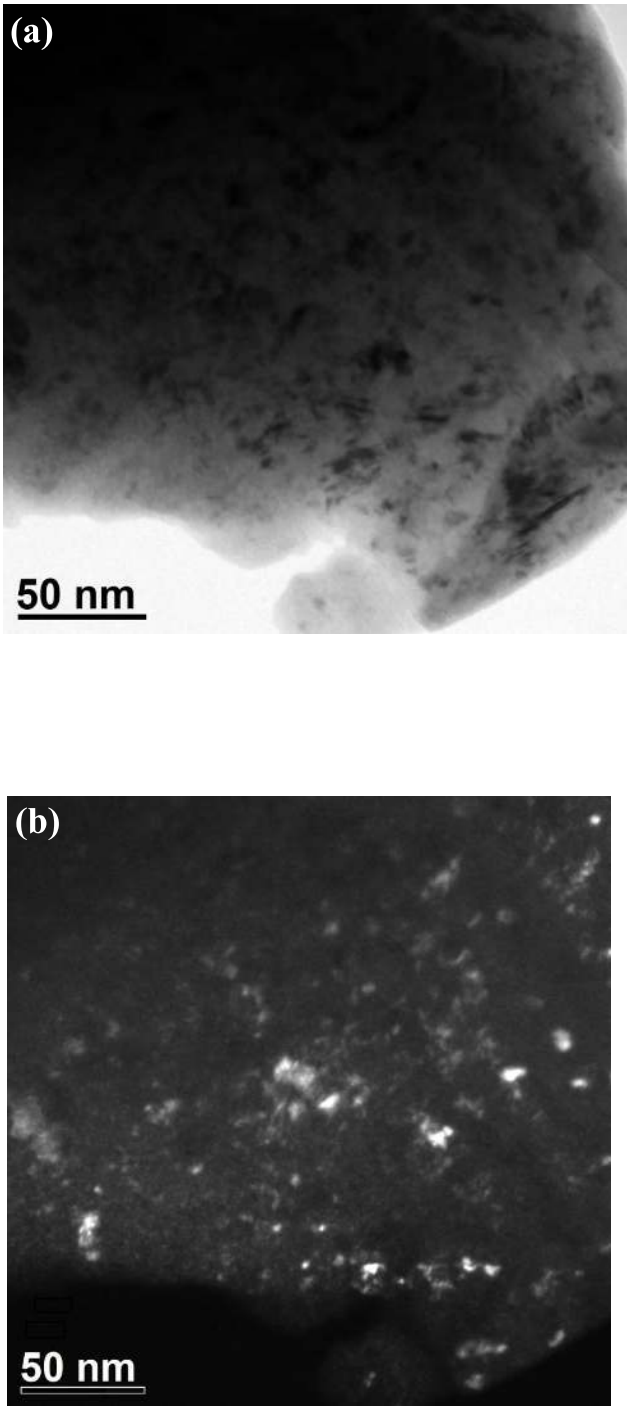

Figure 6.4: (a) Bright field image and dark field image of 50 h milled powder of Al-30 at.% Fe alloy.

Bright field and dark filed image of 50 h milled Al-30 at.% Fe alloy (Fig. 6.4(a) and (b)) reveals the presence of nanocrystalline structure suggesting the presence of nanostructured Al_5Fe_2 intermetallic phase which agrees well with the structural evolution obseved from the XRD pattern.

6.3 Mechanical properties

Microhardness variation with milling time for Al-30 at.% Fe alloy is shown in Fig.6.5. It is apparent from the plot that single Al_5Fe_2 intermetallic phase subjected to MM resulted in Hall–Petch (HP) break down and showed two distinct behaviors. The break-down of Hall-Petch for the averaged hardness can be ascribed to the structural complexities and the deformation mechanism that occur due to mechanical milling. The HP slope decreases below a critical grain size and become negative indicating inverse Hall-Petch (IHP) behaviour. The HP strengthening has been ascribed to the pile-up of dislocations and their resistance to slip transfer. However, since dislocation activity is HP behavior for grain size ranging from 101 to 32 nm and an IHP behavior for grain sizes less than 32 nm was observed. Wadsworth and Nieh [Nieh *et al.* (1991)] predicted that at particular grain size HP relationship would break at which each individual grain in a polycrystalline sample will no longer be able to support more than one dislocation. Theoretically, the critical value of the grain size that can sustain a dislocation pile-up can be predicted from equation 1.9 with $G = E/3$, $v = 0.3$, $b = 1\,nm$ and $H = 8.8\,GPa$, a value of d_c = 8.5 nm was obtained.

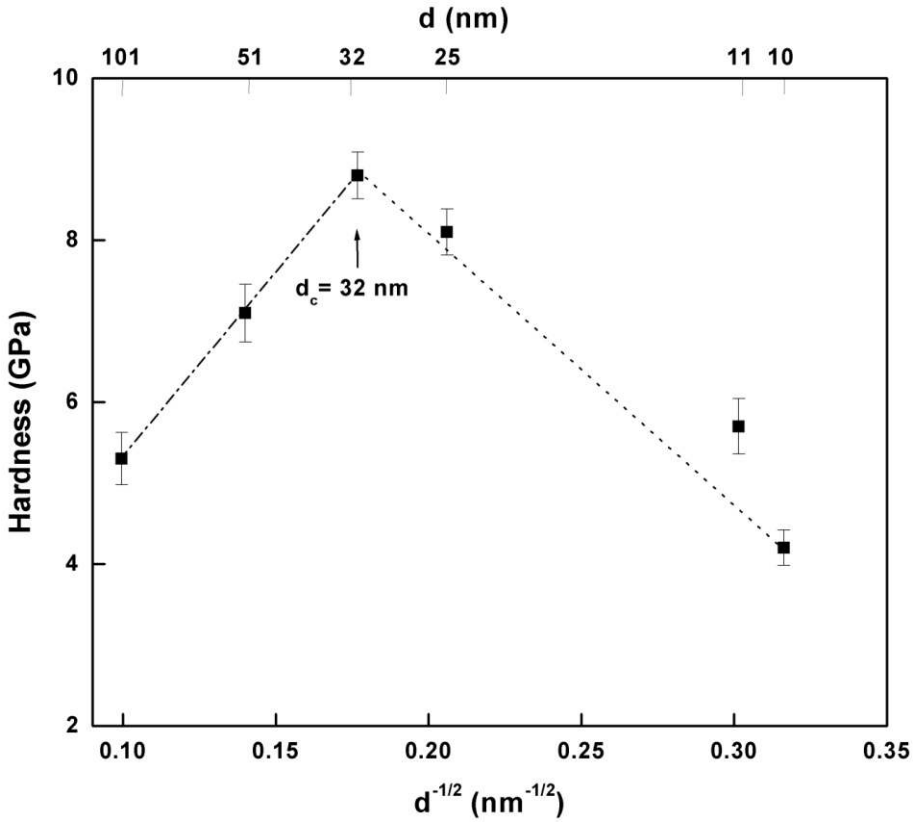

Figure 6.5: Hall-Petch plot of hardness of Al_5Fe_2 intermetallic against inverse square-root of grain size showing transition from conventional Hall-Petch behavior to inverse Hall-Petch behavior.

This critical grain size, 8.5 nm is indeed much lower than experimental value which resulted in 32 nm. Thus the dislocation pile-up mechanism cannot intend the grain size at which HP breakdown occurs. It has been proposed by Weng *et al.* (2003 & 2009)] that the volume fraction of grain boundaries increases noticeably as the grain size decreases to tens to nanometers.

On the other hand the minimum grain size, d_{min}, attainable by milling is the result of a balance between the defect/dislocation structure introduced in the material

by severe deformation of the milling and the recovery via thermal process [Eckert *et al.* (1992)]. It is well-documented that during milling, the grain size decreases with milling time, reaching a minimum grain size, d_{min}, which is a characteristic of each system. Thus the critical grain size achieved during milling is calculated based on a dislocation model [Mohamed (2003)] which states that d_{min} is governed by a balance between the hardening rate introduced by dislocation generation and the recovery rate arising from dislocation annihilation and recombination that predicts the value of d_{min}

Table 6.1: Data for Al_5Fe_2

Parameter	Value
Melting point, T_m (K)	1442
Composition, at.% (at 273K)	Al-30%Fe
Modulus, G (GPa)	61.8
Burger vector (nm)	1
Activation energy [a] (kJ mol^{-1})	172

[a] Average of reported values

as a function of material parameters, such as hardness, melting temperature, and stacking fault energy. The normalized minimum grain size obtainable by milling in terms of hardness is given by the following equation

$$d_{min}/b = A_3\left(e^{-\beta Q/4RT}\right)(D_{PO}Gb^2/v_0kT)^{0.25}\,(\gamma/Gb)^{0.5}(G/H)^{1.25} \quad (6.1)$$

where G is the shear modulus, b is the Burgers vector, γ the stacking fault energy, H the hardness of the material with grain size d and βQ the activation energy for the recovery process. The material parameters used for calculation are presented in

Table 6.1. With the model parameters the d_{min} obtained was around 21 nm which is comparatively larger than the dislocation pile-up model proposed by Wadsworth and Nieh but lower than the experimental value. Thus dislocation models fails to predict the critical grain size and models based on grain boundaries need to be considered.

6.4 Inverse Hall-Petch behavior

Inverse Hall–Petch / grain size softening effect is a phenomenon wherein materials get softer with decreasing grain size. This phenomenon, as it is present in intermetallics, is discussed here. Proposed deformation mechanism based on mesoscopic (≥ a grain diameter) grain / interphase boundary sliding controlled flow, which is confined to the grain / interphase boundary regions and stress-assisted thermally activated motion in the grain boundary in which the deformation rate is produced by independent atomic shear events are accounted as a viable deformation mechanism

6.4.1 Grain boundary sliding

A full account of the model and the validation procedures are available in [Sripathi *et al.* (2012 & 2014), Padmanabhan *et al.* (1996, 2012, 2004 & 2009) and Hahn *et al.* (1997)]. The model considers grain boundary sliding (GBS) that develops to a mesoscopic scale as the rate controlling process. As the model was described only recently [Padmanabhan *et al.* (2014)], in this note only the relevant equations are collated, with minimal explanation to provide the needed physical picture. The rate-controlling mechanism for the occurrence of the IHP effect - mesoscopic grain boundary sliding - is assumed to be confined to the grain / interphase boundary regions [Padmanabhan *et al.* (1996)]. The basic sliding unit is assumed to be an oblate spheroid

in shape of atomistic dimensions (idealized, for easy mathematical treatment) [Eshelby (1957)]. When the basic sliding units in a boundary shear to reach the end, its further deformation is facilitated by a few contiguous boundaries (their number is a function of grain size, temperature and stress) aligning themselves to form plane interfaces (which physically would constitute mesoscopic boundary sliding), a process which gives rise to a long-range (threshold) stress. To know the effective stress driving the deformation, the threshold stress should be subtracted from the applied stress. In the model, plane interface formation is the result of free energy minimization of the total system and the tendency of the external stress to do maximum work in this configuration (principle of maximum work of G I Taylor). By the interconnections of several such shearing plane interfaces large scale sliding can result. The relevant equations are:

$$\dot{\gamma} = \frac{2W\gamma_0 v}{L} \sinh\left(\frac{(\tau-\tau_0)\gamma_0 V_0}{2\,kT}\right) exp\left(-\frac{\Delta F_0}{kT}\right) \tag{6.2}$$

where $\dot{\gamma}$ is the strain rate, L the grain size, γ_0 the mean shear strain associated with a unit-sliding event (~ 0.10 [Wolf (1990)]), ΔF_0 the free energy of activation needed for the basic sliding event, V_0 the volume of the basic sliding unit, which, for this case, is given by $V_0 = (2/3)\pi W^3$, W the grain boundary width (~ 2.5 a_0, where a_0 is the atomic diameter [Haasen (1978)]), v the thermal vibration frequency (10^{13} s^{-1} or (kT/h) s^{-1}, with h Planck's constant), k the Boltzmann constant, T the absolute temperature of deformation, τ the externally applied shear stress and τ_0 is the long-range threshold shear stress necessary to be overcome for the onset of mesoscopic grain / interphase boundary sliding.

$$\Delta F_0 = \frac{1}{2}(\beta_1\gamma_0^2 + \beta_2\varepsilon_0^2)GV_0 \tag{6.3}$$

where G is the shear modulus, $\beta_1 = 0.944\frac{(1.590-p)}{(1-p)}$ and $\beta_2 = \frac{4(1+p)}{9(1-p)}$, with p Poisson's ratio.

$$H_V = H_{Va} - \frac{m_2}{L}(L - L_0)^{1/2} \tag{6.4}$$

where H_V is the measured steady state hardness, H_{Va} is the instantaneous hardness recorded on load application and L_0 is the grain size at which τ_0 will be zero ($= 2\sqrt{6}W$ [Hahn *et al.* (1997) and Venkatesh *et al.* (1996)]). m_2 and L_1 are defined as:

$$m_2 = \frac{GL_1^{1/2}}{C} \qquad L_1 = 2^{3/2}3^{-3/4}N^{-1/2}\frac{\gamma_B}{G\alpha_f} \tag{6.5}$$

where C is a conversion factor (from shear to hardness; depends on the yield criterion used), α_f a form factor of the order of unity (to account for the real shape of the basic sliding unit, if it is different from an oblate spheroid), γ_B the specific grain-boundary energy and N is the number of grain boundaries participating in a mesoscopic sliding event. From equation, 6.5, it follows that m_2 is the slope of the hardness versus $(L - L_0)^{0.5}/L$ plot. Therefore, using experimental hardness - grain size data and this equation, L_1 and N can be computed.

The threshold stress, in turn, is calculated as [Padmanabhan *et al.* (2004)]:

$$\tau_0 = G\left[\frac{L_1}{L}\left(1 - \left(\frac{L_0}{L}\right)\right)\right]^{0.5}, \text{ L}\geq\text{L}_0 \tag{6.6}$$

Using this value of τ_0, the free energy of activation, ΔF_0, from equation 6.3 was calculated.

6.4.2 Thermally activated grain boundary shearing

Conrad and Narayan [Conrad *et al.* (2000)] proposed that during the deformation of nanocrystalline materials, the controlling process is stress-assisted thermally activated motion in the grain boundary in which the deformation rate is produced by independent atomic shear events (atomic jump processes). Under this condition, they developed the rate-controlling equation given by equation 1.13 [Conrad *et al.* (2000)]:

$$\dot{\gamma} = \frac{6bv_D}{d}\sinh\left(\frac{v\tau_e}{kT}\right)exp\left(-\frac{\Delta F}{kT}\right)$$

Expansions of parameters according to [Conrad *et al.* (2000)] are: v_D the Debye frequency ($\approx 10^{13}s^{-1}$), grain boundary width $\approx$ 3b, where b the atomic diameter, effective shear stress, $\tau_e = \tau - \tau_c$ where τ is applied stress and τ_c is the threshold or critical stress, ΔF is equal to the activation energy for grain boundary diffusion, v the activation volume equals b^3, k the Boltzmann constant and T temperature on absolute scale. For calculations the parameters takes the following values, the shear rate $\dot{\gamma} = 10^{-3}s^{-1}$ and by assuming ($\tau_c = 0$), $\tau_e \approx \tau$, where $\tau = H/3\sqrt{3}$. Equation 1.13 can be expressed in two different forms in terms of hardness by approximating the pre-exponential stress function contained in sinh function [Conrad *et al.* (2002)] as

$$H = 3\sqrt{3}\left\{\left[\frac{kT}{v}ln\left(\frac{\dot{\gamma}}{bv_D}\right) + \frac{\Delta F}{kT} + lnd\right]\right\} \quad (6.7)$$

$$H = 3\sqrt{3}\left\{\frac{kT}{v}\left[\left(\frac{\dot{\gamma}}{3bv_D}\right)exp\frac{\Delta F}{kT}\right]\right\}d \quad (6.8)$$

The model was validated for IHP regime of the current experimental data and the experimentally observed and calculated hardness values of this system are shown in

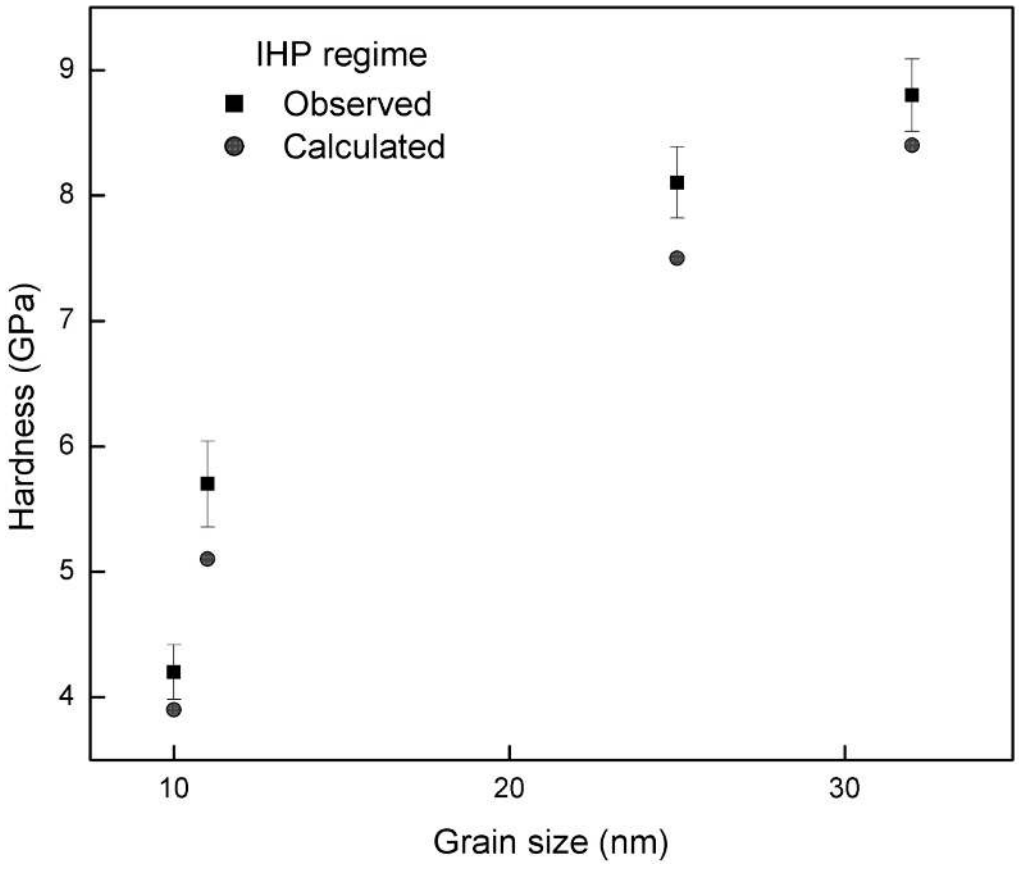

Figure 6.6: Hardness vs grain size in IHP regime observed values and calculated values obtained using equation 6.8.

Fig. 6.6. The degree of fit, as described by coefficient of correlation, for all the three expressions H_v vs. ln(L), H_v vs. L (these two describe the rigorous and approximate forms of the relationship in the model of Conrad and Narayan [Conrad *et al.* (2000)] and H_v vs. $(L\text{-}L_0)^{0.5}/L$ [Padmanabhan *et al.* (2014)] is very similar and the findings are presented in Table 6.2. On this basis, both the models are acceptable.

The preceding discussion shows that although the model proposed by Conard and Narayan explains the IHP effect the parameters used for validation is quite unreasonable (a) the effective stress is taken equal to the applied stress, i.e., the strain-rate sensitivity index, m = 1.0. But, in nanocrystalline materials at room temperature the value of m is in the range of 0.02-0.08 [Padmanabhan (2001) and Varam *et al.* (2014)] and (b) Further the strain rate was assumed as $10^{-3}s^{-1}$ but according to [Maier *et al.* (2011)] strain rate lies in the range of $5x10^{-2}s^{-1}$ to $5x10^{-4}s^{-1}$.

Table 6.2: Degree of fit for the three relations: $H_v \alpha \ln(L)$, $H_v \alpha L$ and $H_v \alpha (L\text{-}L)^{0.5}/L$

System	L, nm	H, GPa	Correlation coefficient of H and		
			ln(L)	L	$(L\text{-}L)^{0.5}/L$
Al_5Fe_2	32.0	8.8	0.970	0.949	0.968
	23.6	8.1			
	11.0	5.7			
	10.0	4.2			

Thus the experimental data was analyzed using both the strain rate values and the free energy of activation, ΔF_0, for the rate controlling process (mesoscopic GBS) and refined values of γ_0 were determined as a function of strain rate and the results are presented in Table 6.3. Algorithm developed for validating the mesoscopic GBS controlled flow model for inverse Hall-Petch effect is given in Appendix A. The following observations are interesting: The relative change in hardness as one goes from the HP to the IHP region is much less in intermetallics than in nanocrystalline materials. This aspect needs further study. But it is clear that the observed IHP effect in intermetallics also could be explained in terms of the mesocopic grain boundary sliding

controlled flow process, as with the other classes of materials. Finally, as the value of N for all the systems (Table 6.3) is less than one, it follows from the model

Table 6.3: Average shear strain in the basic unit of sliding, the number of grain boundaries that align to form a plane interface during mesoscopic boundary sliding and the free energy of activation for the rate controlling GBS process.

System	N	L, nm	τ_0, GPa	γ_0, refined *	$\Delta F_0, kJ/mol$	
					$\dot{\gamma} = 5X10^{-2}, s^{-1}$	$\dot{\gamma} = 5X10^{-4}, s^{-1}$
Al_5Fe_2	0.8458	32.0	1.52	0.0711	157.73	170.37
		23.6	1.74			
		11.0	2.27			
		10.0	2.33			

G = 61.8GPa

*As the strain rates in the indentation tests are assumed to be in the range of $5 \times 10^{-2}\ s^{-1}$ to $5 \times 10^{-4}\ s^{-1}$ [Maier *et al.* (2011)], refined γ_0 values were obtained for the mean values of ΔF_0 for this range.

[Padmanabhan *et al.* (1996 & 2004) and Venkatesh *et al.* (1996)] that plane interface formation in these intermetallics of the studied grain size ranges is the result of dislocations/ partial dislocations being emitted from the deforming boundary, which then traverse the grain and get absorbed at the opposite boundary [Padmanabhan *et al.* (1996 & 2004)].

6.5 Conclusions

1. High energy ball milling of Al_5Fe_2 resulted from Al-30%Fe alloy resulted in the formation of nanocrystalline intermetallic and found quite stable under the present

experimental conditions and crystallite size of it decreases up to 10 nm with an increase in milling time.

2. Microhardness measurements of single Al_5Fe_2 nanocrystalline intermetallic phase produced by mechanical milling resulted in Hall–Petch (HP) break down and showed two distinct behaviors. The break-down of HP for the averaged microhardness measurements was found to be due the transition of deformation mechanism from dislocation activity to grain boundary sliding.
3. Dislocation models could not intend the critical grain size at which the HP relation breakdown and so models based on grain boundaries were considered.
4. Detailed analysis showed that models based on grain boundaries namely grain boundary sliding and thermally activated grain boundary shearing seems to be reasonable in explaining the IHP effect.
5. Grain boundary sliding is ascribed to be a viable deformation mechanism resulting in softening behavior observed in this system.